

# Heterogeneous $\text{NH}_4\text{ClO}_4$ Decomposition Using Isothermal and Pulsed Laser Mass Spectrometry

G. L. PELLETT\*

*Langley Research Center, Hampton, Va.*

A pulsed ruby laser-mass spectrometry technique was developed and applied, wherein granular mixtures of ammonium perchlorate (AP) and light-absorbing substrate materials were rapidly flash pyrolyzed (0.8 ms) within the low-pressure ion source chamber of a Bendix TOF Mass spectrometer. Gaseous products from AP mixed with carbon black, copper chromite,  $\text{Fe}_2\text{O}_3$ , and  $\text{MnO}_2$  indicated a predominance of high-temperature heterogeneous reactions. The first step appeared to be proton transfer dissociation of AP into  $\text{NH}_3$  and  $\text{HClO}_4$ . Adsorbed  $\text{HClO}_4$  underwent rapid heterogeneous decomposition on the substrate material;  $\text{ClO}_2$  and  $\text{HCl}$  were evolved as major products, but  $\text{ClO}_3$ ,  $\text{ClO}$ , and  $\text{Cl}_2$  were only minor products. Chemisorbed oxygen and oxygen carriers such as  $\text{OH}$  and  $\text{ClO}$  were likely formed on the substrate simultaneously, however. These could react with adsorbed  $\text{NH}_3$  and its dehydrogenated fragments to form  $\text{H}_2\text{O}$ ,  $\text{NO}$ , and  $\text{HOCl}$  as major gaseous products;  $\text{N}_2$ ,  $\text{N}_2\text{O}$ , and  $\text{NO}_2$  were minor products. Low-pressure isothermal decompositions of AP and AP/substrate mixtures in a glass capillary were utilized to compare product distributions. The site of  $\text{HClO}_4$  decomposition (crystal vs substrate surface) was concluded to be at least as important as temperature and effective residence time in determining the predominant chemical pathways.

## Introduction

DESPITE several hundred investigations on the decomposition and deflagration of ammonium perchlorate<sup>1</sup> and other solid-propellant ingredients over the past 15 years, there has been a notable scarcity of high-temperature pyrolysis studies that provide significant chemical information on the rapid gasification of deflagrating solids. The laser pyrolysis-mass spectrometry (LP) approach was developed in an attempt to satisfy certain aspects of this need. In particular, the present use of a pulsed ruby laser permitted selective study of heterogeneous reactions that occur when hot substrates (light-absorbing) contact  $\text{NH}_4\text{ClO}_4$  (AP) and rapidly surface-heat the oxidizer by conduction.

The high-vacuum environment of the mass spectrometer ion source chamber, under which AP/substrate mixtures and other AP-based ingredients were pyrolyzed, was obviously not a practical condition for deflagration. The arrangement did, however, serve to eliminate several gas sampling problems and thus permit direct analyses of primary gaseous products, evolved from solid-phase and interfacial condensed-phase reactions, in the absence of complicating gas-phase diffusion and reaction effects.

The application of a pulsed laser as an intense heating source is especially suited to mass spectrometer pyrolyses at temperatures where the rate of volatilization is high. Slower methods of heating can produce large quantities of gaseous products during heat-up which "flood" a mass spectrometer before the desired temperature is attained. An important advantage of the laser application is the possibility of optimizing sample geometry and avoiding physical contact between the sample and reactive boundaries, as in heated capillaries, hot stages, or resistance-heated filaments. The

monochromatic character of the laser often precludes a number of undesirable photochemical reactions.

The ruby laser used in the present LP studies exerted two main constraints on the experimental conditions, however. First, the relatively fixed pulse shape of 0.8 msec duration prevented an experimental study of time and total-energy effects at constant heating rate. Secondly, different optical absorbances of mixture components at 6943 Å (AP absorbs weakly) resulted in differential heating and variable light absorption in-depth. Although the absorbance differences were utilized advantageously to favor heterogeneous reaction pathways in the present AP system, both of the above "constraints" have been circumvented recently by using a  $\text{CO}_2$  gas laser,<sup>2</sup> which emits at 10.6  $\mu\text{m}$  (where AP absorbs strongly) and has a widely variable square-pulse duration and power output.

## Experimental

### Materials and Characterization

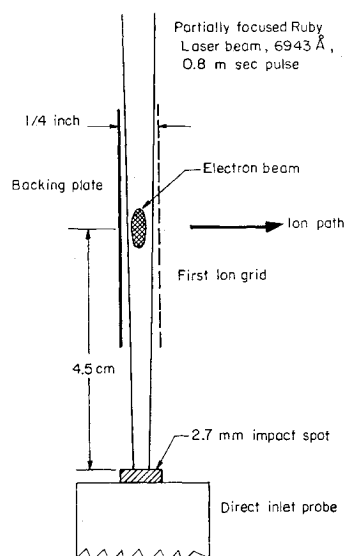
The ammonium perchlorate (AP) was a finely ground commercial grade, with particle size averaging about 30  $\mu\text{m}$ . Initial exploratory LP were also carried out with Matheson-Coleman-Bell reagent grade material, finely ground; no differences in product distributions were noted. The carbon black was Fisher reagent grade, of particle size 1  $\mu\text{m}$  or smaller. LP of this material yielded relatively small peaks due to  $\text{H}_2\text{O}$ ,  $\text{CO}$ , and  $\text{CO}_2$ , and a somewhat smaller peak at mass 26. The copper chromite was Harshaw-Chemical Cu 0202, having a nominal composition of 82%  $\text{CuO}$ , 17%  $\text{Cr}_2\text{O}_3$ , and 1% impurities, and an average particle size of about 2  $\mu\text{m}$ . The  $\text{Fe}_2\text{O}_3$  and  $\text{MnO}_2$  were reagent grade, having average particle sizes of about 1.5  $\mu\text{m}$  and 80  $\mu\text{m}$ , respectively.

To assure uniformity and satisfactory mixing, mixtures were lightly ground in a mortar just before use. Samples were lightly packed in a small aluminum dish and degassed in the mass spectrometer for at least  $\frac{1}{2}$  hr. LP of the metal oxides yielded mainly  $\text{O}_2$  and smaller amounts of  $\text{H}_2\text{O}$ . The  $\text{O}_2$  evolved was sufficiently large to preclude reporting of accurate product  $\text{O}_2$  values from LP of AP/metal oxide mixtures. Corrections for the excess  $\text{H}_2\text{O}$  evolved (estimated to be 10-20%) were not made in reporting product  $\text{H}_2\text{O}$ .

Presented as Paper 68-149 at the AIAA Sixth Aerospace Sciences Meeting, New York, January 22-24, 1968; submitted February 14, 1968; revision received February 16, 1970. The author gratefully acknowledges stimulating discussions with A. R. Saunders, the skillful experimental assistance of W. R. Cofer, III and G. C. Purgold, and the manuscript and figure preparation by J. LaNeave and N. Kemper.

\* Aero-Space Technologist, Propulsion Branch, Applied Materials and Physics Division. Member AIAA.

**Fig. 1 Sampling configuration within low-pressure ion source chamber of Bendix TOF.**



### Apparatus

The sampling configuration is shown in Fig. 1. The partially focused pulsed laser beam entered the Model 14 Bendix TOF mass spectrometer ion source chamber vertically to impact samples about 45 mm below the electron beam. The basic optical system employed a 76-cm laser-to-sample distance, a moderately divergent  $9.5 \times 102$  mm ruby rod (about 7 millirad) with reflective dielectric coatings on both ends, partial focusing with a 20-cm focal length lens, and defining apertures positioned before and after the lens.

A fixed 4-joule output pulse of 0.8 msec duration was used from the 20-joule ruby laser (Korad K-1) in order to maintain the same relative pulse shape and minimize long-term output degradation. Calibrated transmission filters (at 6943 Å) were used to vary the delivered impact energy, which generally ranged from about 2 to 10 cal/cm<sup>2</sup>, depending on the sample.

Qualitative estimates of the surface distribution of impact energy were made by examining impacts on unexposed Polaroid film. A reproducible central spot of about 2.7 mm diam received a reasonably uniform distribution of energy (probably within  $\pm 15\%$ ); it was surrounded by an annular region in which the energy decreased radially to a sharp cut-off at about 3.5 mm.

The development of excessive pressures in the ion source region was alleviated by removing the standard pumping baffle, which opened up the entire cross section of the flight tube between the ion source and liquid  $\text{N}_2$  trap/Hg diffusion pump system. Initial pressures were  $<10^{-6}$  torr.

### Discussion of Laser Pyrolysis Technique

The LP technique represents a new approach to the study of heterogeneous reactions between AP and various binder matrix constituents. The predominance of heterogeneous reaction pathways was determined primarily by the effective transparency of AP to 6943 Å light, and the relatively short heating pulse.<sup>†</sup> Impact energies in excess of 60 cal/cm<sup>2</sup> were required to produce a minimal mass spectrum with AP only. Thus when AP was flashed at much lower energies while in contact with light-absorbing carbon black or metal oxide catalysts, the substrate became preferentially heated and the dissociation/decomposition initially ensued at the hot substrate-AP interface. Subsequently, evolved gases caused particle separation effects to occur, new contact inter-

faces were established, and some of the product gases reacted with hot substrate particles.

It will be indicated later that, with the exception of  $\text{HClO}_4$  and  $\text{NH}_3$ , the  $\text{HCl}$ -normalized gaseous product ratios were relatively insensitive to laser impact energy over threefold ranges. The reasons for this are unclear presently, although it seems plausible to consider temperature regulatory mechanisms such as a quasi-equilibrium vaporization and/or an effective particle contact time that decreases with increasing substrate temperature.

A few continuous time histories of product evolution rates from LP were measured by displaying the single-peak output of a Bendix 3012 analog. The smoothed results of ten laser impacts on a 5%  $\text{Fe}_2\text{O}_3/\text{AP}$  mixture are shown in Fig. 2, where the ion current intensities (proportional to evolution rate) were normalized to 100 and the laser peak power to 40. The laser pulse began at about 0.5 ms after triggering. With the exception of  $\text{HOCl}$ , all the product ion intensities began to rise at about 1.0 ms and peaked at about 2.4 ms. The respective half-peak time durations were 2.2, 4.0, and 19 ms for  $\text{HClO}_4$ ,  $\text{NH}_3$ , and  $\text{H}_2\text{O}$ .  $\text{HCl}$ ,  $\text{ClO}_2$  (corrected for electron-impact fragmentation of  $\text{HClO}_4$ ) and  $\text{NO}$  exhibited time histories similar to  $\text{H}_2\text{O}$ .  $\text{HOCl}$  did not begin its rise until about 3 msec.

The usual method of data recording consisted of photographing the entire mass spectrum (30 kHz repetition rate) as it was displayed on a short-persistence phosphor oscilloscope from time zero up to a preselected time. Good photographic spectra were easily obtained in 2 msec or longer, which provided a check on product evolution histories. With 40 msec spectra, used most frequently to assure a complete time-averaged record, the measured mass peak heights corresponded to values of the maximum ion intensities attained; e.g., those seen in Fig. 2 at 2.4 msec. Under the present sampling conditions these reported ion intensities were considered to be approximately proportional to the respective maximum rates of product evolution.

Throughout the LP work each sample mixture was impacted sequentially up to 20 times, at varying energies, with each laser flash progressively deepening the impact crater. The lower limit of impact energy was generally that required for a readable mass spectrum; the upper limit corresponded to a condition where "flood out" and possible damage to the mass spectrometer were imminent. It was generally possible to explore a threefold energy range with each sample.

### Treatment of Data

When the major pyrolysis products from sequences of up to 20 impacts were normalized with respect to  $\text{HCl}$ , the resulting product ratios were generally quite independent of impact number and also of laser impact energy, within the single-impact ratio error limit of about  $\pm 15\%$ . Two exceptions,

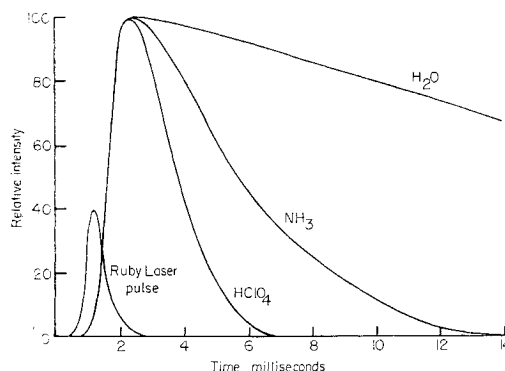


**Fig. 2 Time dependence of product evolution in laser pyrolysis of a 5%  $\text{Fe}_2\text{O}_3/\text{NH}_4\text{ClO}_4$  mixture.**

<sup>†</sup> Results from our  $\text{CO}_2$  laser pyrolysis technique<sup>2</sup> fully support the aforementioned dominance of heterogeneous reaction pathways.

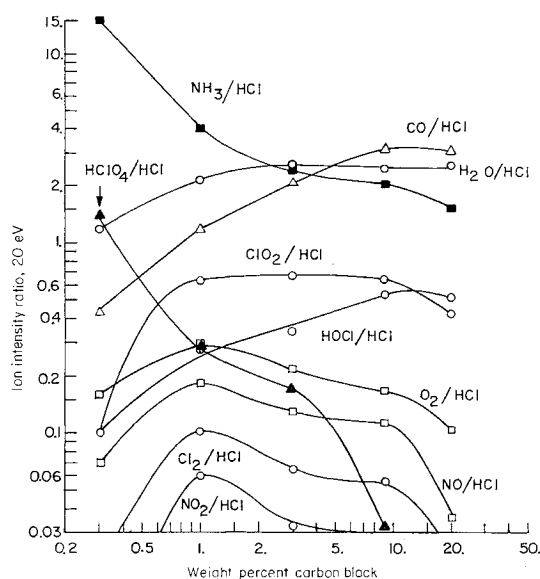


Fig. 3 Ruby laser pyrolyses of  $\text{NH}_4\text{ClO}_4$ /carbon black mixtures.

however, were normalized  $\text{HClO}_4$  and  $\text{NH}_3$ , which increased sometimes with impact number and decreased with increasing impact energy.

In cases where  $\text{HClO}_4$  was evolved in relatively large quantities,  $\text{ClO}_2$  ion due to electron impact of  $\text{HClO}_4$  had a relatively short appearance time compared to product  $\text{ClO}_2$ . The latter could be read directly by excluding the less-intense transient peak contribution from  $\text{HClO}_4$  fragmentation. In other cases where  $\text{HClO}_4$  was evolved in small quantities, the product  $\text{ClO}_2$  peak was as intense and well defined as other stable product peaks. In some instances  $\text{ClO}_2/\text{HCl}$  exhibited a slight tendency to decrease with increasing impact energy, but to a much lesser extent than  $\text{HClO}_4$ .

After several hundred LP results were compared over a wide range of sample compositions, it appeared justifiable to report only numerical averages of  $\text{HCl}$ -normalized product ratios obtained from 10 to 20 successive LP on a sample at different energies. Note that the special characteristics of  $\text{HClO}_4$  and  $\text{NH}_3$  evolution (short-lived and energy-sensitive) preclude absolute comparisons with other specie measurements.

## Results

### LP of AP/Carbon Black System

The AP/carbon black system was studied to serve as one type of reference. It was thought that purely thermal decomposition pathways should compete favorably with reactions otherwise catalyzed by direct oxygen exchanges and/or electron transfer processes characteristic of transition metal oxides.

Averaged gaseous product distributions from LP of different weight percent carbon black/AP mixtures are shown in Fig. 3. Note that the products of dissociative evaporation,  $\text{NH}_3$  and  $\text{HClO}_4$ , decreased in relative abundance with increasing carbon black. In a sense these may be considered primary reactants. Since a 3.1  $\text{NH}_3/\text{HClO}_4$  ion intensity ratio (20 eV) corresponded to a unity mole ratio (in low-pressure heated-capillary pyrolyses of AP decomposition residues), there was also a large stoichiometric deficiency of evolved  $\text{HClO}_4$ , compared to  $\text{NH}_3$ , throughout. Similar deficiencies were seen in the AP/metal oxide systems (presented later). Although some preferential desorption of  $\text{NH}_3$  (over adsorbed  $\text{HClO}_4$ ) is attributable to the transient heating behavior of AP under vacuum conditions (see Ref. 2), these results obviously reflect the lower thermal stability characteristic of adsorbed  $\text{HClO}_4$ .

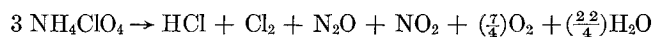
Inspection of the product distributions in Fig. 3 indicates that the extent of  $\text{HClO}_4$  decomposition and  $\text{NH}_3$  oxidation increased strongly with added carbon black. Note especially that  $\text{ClO}_2$  and  $\text{HOCl}$  emerged as characteristic heterogeneous decomposition products.  $\text{CO}$  became increasingly abundant, indicating substrate oxidation, and the  $\text{CO}_2/\text{HCl}$  product curve (not shown) coincided closely with  $\text{ClO}_2/\text{HCl}$ . It was surprising that  $\text{O}_2$ ,  $\text{Cl}_2$ , and  $\text{NO}_2$  were not very abundant. These results contrast sharply with isothermal decompositions of AP, where all three were major products of condensed-phase decomposition (presented later). LP of AP crystals spread on a graphite substrate yielded product distributions much the same as those shown for the 1–9% carbon black systems, thus further supporting the concept of heterogeneous interfacial reactions initiated at hot substrate/AP interfaces.

Results were also obtained from LP of a 30% (estimated) carbon black/ $^{15}\text{NH}_4\text{ClO}_4$  mixture, where  $\text{N}_2$  and  $\text{N}_2\text{O}$  were mass separated from  $\text{CO}$  and  $\text{CO}_2$ , respectively. The 20 eV ion intensity ratios, normalized to  $\text{HCl} = 1.00$ , were  $\text{N}_2 \cong 0.1$ ,  $\text{CO} = 2.9$ ,  $\text{N}_2\text{O} \cong 0.05$ ,  $\text{CO}_2 = 0.76$ ,  $\text{NO} < 0.1$ ,  $\text{NO}_2 < 0.01$ ,  $\text{ClO}_2 = 0.31$ ,  $\text{HOCl} = 0.44$ , and  $\text{O}_2 < 0.1$ . From this, and also some LP of  $^{15}\text{NH}_4\text{ClO}_4$  on graphite, it appeared that neither  $\text{N}_2$  nor  $\text{N}_2\text{O}$  were major decomposition products in the AP/carbon black system.

Ion intensities of the  $m/e = 14, 15$  peaks were always negligibly small in comparison to  $\text{NH}_3$  ( $\sim 1\%$ ), so that  $\text{N}$  and  $\text{NH}$  can be ruled out as significant gaseous products in the carbon black and also metal oxide/AP systems. The average  $\text{NH}_2/\text{NH}_3$  ion intensity ratio (20 eV) in the carbon black/AP system was 0.27, compared to nearly constant values of 0.31 and 0.30 in isothermal pyrolyses of AP decomposition residues at 260 and 380°C. Thus most of the  $\text{NH}_2$  ion observed was probably due to electron-impact of  $\text{NH}_3$ .

### Isothermal Decompositions (ID) of Pure AP

Results from LP of AP/carbon black mixtures were notably different from previous low external pressure ( $10^{-6}$  torr) ID of AP in a Bendix TOF mass spectrometer. In the ID studies, loosely packed samples of reagent grade AP were pyrolyzed in a  $9 \times 1$  mm filament-heated glass capillary, positioned 25 mm below the ionizing electron beam.† Fragmentation patterns, and with the exception of  $\text{H}_2\text{O}$ , relative sensitivities were determined experimentally from pure gases to calculate ID mole ratios from 70 eV ion intensities. The time-independent condensed-phase decomposition product ratios are plotted vs temperature in Fig. 4. At 200°C the results were well accounted for by



Minor products ( $< 0.1 \text{ Cl}_2$ ) in these cases were  $\text{N}_2$ ,  $\text{NO}$ , and  $\text{ClO}_2$ .

Figure 4 also shows more recent low-pressure ID results calculated from 20 eV data by using empirically determined (matched in overlap region) sensitivity factors. Relatively small but increasing quantities of  $\text{NO}$  and  $\text{N}_2$  (not shown) were formed at temperatures above 300°C. Note that the above results were obtained at much lower pressures than used previously,<sup>3–5</sup> so that desorption and primary condensed-phase reactions were favored over secondary reaction effects.

Of the six major products of condensed-phase decomposition, from ID of AP, only  $\text{H}_2\text{O}$  and  $\text{HCl}$  were major products in LP of carbon black and metal oxide/AP mixtures; the same conclusion holds for high-temperature  $\text{CO}_2$  laser pyrolyses of pure AP.<sup>2</sup> This fact by itself suggests that significant

† The effective absence of electron-impact decomposition of 1) the solid sample and 2) any AP sublimate formed in the ion source, was demonstrated. The strong appearance of  $\text{NH}_3$  and  $\text{HClO}_4$  only in late ID stages (from postdecomposition AP residue), ruled out 2, and also eliminated thermal cracking of  $\text{HClO}_4$  by the ion source hot filament as a significant "source of decomposition products."

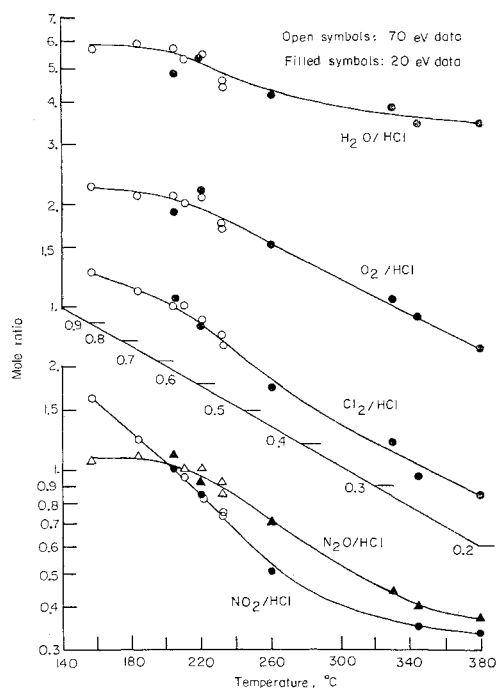


Fig. 4 Condensed-phase decomposition products of  $\text{NH}_4\text{ClO}_4$  heated in a glass capillary at low pressure within ion source chamber of Bendix TOF.

basic differences existed in the respective decomposition mechanisms.

A dominant feature of the ID results for AP was the systematic increase in HCl mole fraction with temperature. Some of the increase at higher temperatures (say,  $>260^\circ\text{C}$ ) was likely due to heterogeneous  $\text{HClO}_4$  decomposition on the glass capillary wall. However, comparisons of sequential results at  $380^\circ\text{C}$  indicated that  $\text{Cl}_2/\text{HCl}$  decreased only from 0.30 to 0.26 while  $\text{HClO}_4/\text{HCl}$  ion ratio increased from 0.1 to 3 before pyrolysis of the decomposition residue (AP) was complete. Although the application of equilibrium considerations to heated-capillary AP decompositions is of questionable validity, it is notable that the Deacon equilibrium,  $\text{H}_2\text{O} + \text{Cl}_2 \rightleftharpoons 2\text{HCl} + \frac{1}{2}\text{O}_2$ , strongly favors the observed decrease in  $\text{Cl}_2/\text{HCl}$  with increasing temperature, at constant pressure. Pressure effects are considered next.

A comparison of AP products in Fig. 4 with others obtained at pressures of several torr<sup>4-5</sup> indicates a two-to-fourfold increase in  $\text{Cl}_2/\text{HCl}$  mole ratio with increased pressure, at  $225^\circ$  to  $300^\circ\text{C}$ . Although the reported values<sup>4-5</sup> are somewhat uncertain, due to incomplete product separation and secondary reactions during isolation and wet-analysis of the "nonvolatile (at  $-78^\circ\text{C}$ ) residue," our comparatively lower  $\text{Cl}_2/\text{HCl}$  suggests that much of the present "excess" HCl would probably undergo condensed-phase oxidation to  $\text{Cl}_2$  at higher pressures; i.e., where desorption is effectively slower, and the Deacon equilibrium favors an increase in  $\text{Cl}_2/\text{HCl}$ .

The absence of significant quantities of  $\text{ClO}_2$  (and  $\text{HOCl}$ ) during ID of AP up to  $380^\circ\text{C}$ , and also during high-temperature  $\text{CO}_2$  laser pyrolyses of AP,<sup>2</sup> is considered relevant, especially since  $\text{HClO}_4$  was also evolved in significant quantities; i.e., the decomposition of adsorbed  $\text{HClO}_4$  on preferred AP crystal sites apparently favors  $\text{Cl}_2$  formation and evolution over  $\text{ClO}_2$  evolution. Note that desorption of  $\text{ClO}_2$  from the AP should not have been a limiting factor since both  $\text{Cl}_2$  and  $\text{ClO}_2$  were significant products during ID of  $\text{KMnO}_4$ -doped AP (presented later).

The LP of AP/metal oxide mixtures are now presented, followed by a summary of characteristic features and interpretations that were found applicable to all the AP-mixture systems.

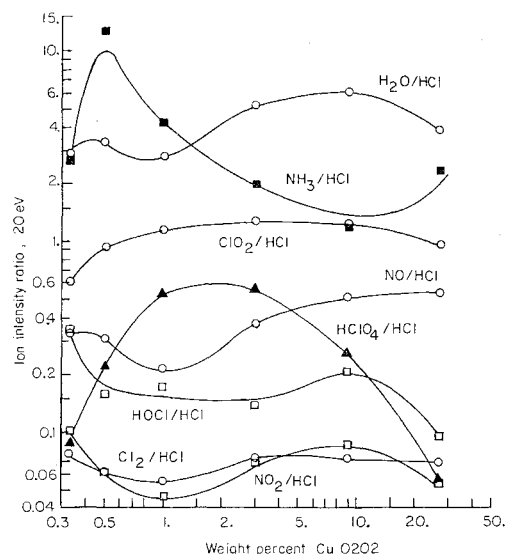


Fig. 5 Ruby laser pyrolyses of  $\text{NH}_4\text{ClO}_4$ /Copper chromite mixtures.

#### LP of AP/Metal Oxide Systems

Averaged gaseous product distributions from LP of AP/copper chromite ( $\text{CuO}2\text{O}_2$ ),  $\text{Fe}_2\text{O}_3$ , and  $\text{MnO}_2$  mixtures are shown in Figs. 5-7, respectively. Other possible products in the  $m/e$  range 2-200 were either nonexistent or detected in very small quantities ( $\text{N}_2$ ,  $\text{N}_2\text{O}$ ,  $\text{ClO}$ , and  $\text{ClO}_3$  are discussed later). Although the product ratios varied significantly with metal oxide type and percentage, the results had a number of features in common. Note in particular that 1)  $\text{HClO}_4$  generally exhibited a large stoichiometric deficiency in the gas phase, compared to  $\text{NH}_3$ , 2)  $\text{H}_2\text{O}$  was the predominant reaction product, and its relative abundance tended to correlate with NO except at very high substrate additions, 3) the concentrations of  $\text{ClO}_2$  and  $\text{HCl}$  usually exceeded  $\text{Cl}_2$  by an order of magnitude, 4) NO predominated over  $\text{NO}_2$  by a substantial margin (expected at high temperatures), and 5)  $\text{HOCl}$  was always significant and characteristic product of heterogeneous decomposition.

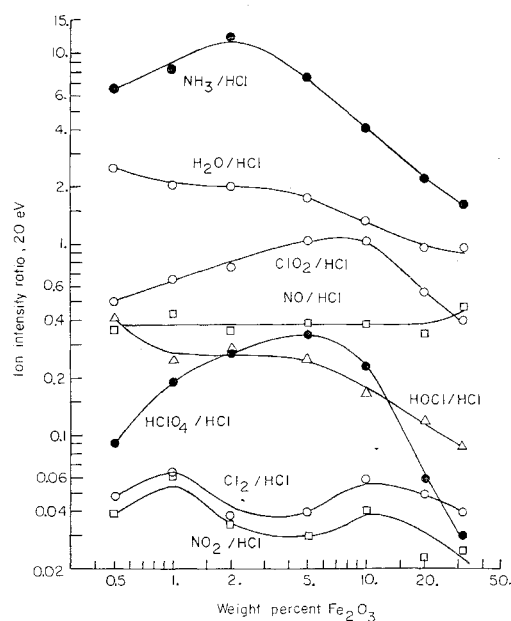


Fig. 6 Ruby laser pyrolyses of  $\text{NH}_4\text{ClO}_4$ / $\text{Fe}_2\text{O}_3$  mixtures.

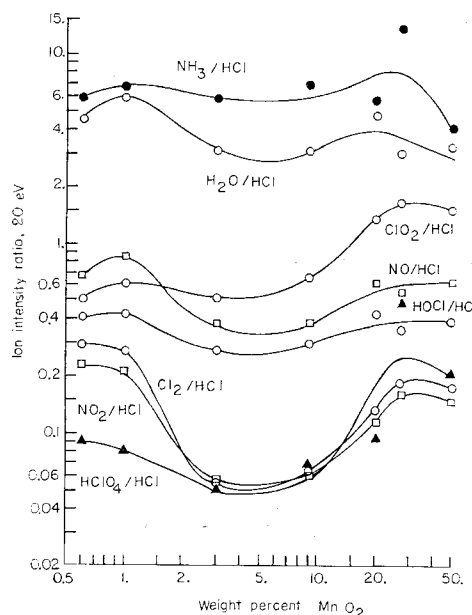


Fig. 7 Ruby laser pyrolyses of  $\text{NH}_4\text{ClO}_4/\text{MnO}_2$  mixtures.

Although  $\text{ClO}$  ion was always observed and measured, the relative abundance of  $\text{ClO}$  radical appeared to be quite small. Corrected  $\text{ClO}/\text{HCl}$  ion ratios§ varied significantly (0–0.02 to 0.16) with mixture composition, but tended to correlate quite well with respective  $\text{Cl}_2/\text{HCl}$  data in the AP/metal oxide and carbon black systems. Corrected  $\text{ClO}/\text{Cl}_2$  ion ratios averaged  $1.15 \pm 0.5$ , based on the 17 most reliable determinations out of a possible 25 in Figs. 3, 5–7.

Some early product distributions obtained from LP of ground  $^{15}\text{NH}_4\text{ClO}_4/\text{metal oxide}$  mixtures are shown in Table 1, in which  $\text{N}_2$  and  $\text{N}_2\text{O}$  were mass-separated from  $\text{CO}$  and  $\text{CO}_2$ , respectively. Although the mixtures were somewhat high in metal oxide concentration, compared to those in Figs. 5–7, the results generally indicate that  $\text{N}_2$  and  $\text{N}_2\text{O}$  were minor decomposition products.

#### Generalizations on LP of AP/Substrate Mixtures

The following generalizations and interpretations characterize some of the more important mechanistic features of the LP results from carbon black,  $\text{CuO}$ ,  $\text{Fe}_2\text{O}_3$ , and  $\text{MnO}_2/\text{AP}$  mixtures.

The primary driving force for decomposition was conduction of heat to AP particles from laser-heated substrate particles. Gas-solid heterogeneous reactions probably predominated after the onset of AP gasification. The characteristic product evolution time histories (typified by Fig. 2) and distributions obtained in this work, and also Ref. 2, indicate that 1)  $\text{HClO}_4$  and  $\text{NH}_3$  can be considered “primary reactants” during ruby LP, 2) subsequent heterogeneous decomposition was very rapid, and presumably occurred at high temperatures, and 3) preferential adsorption/decomposition of  $\text{HClO}_4$  on the substrate generally occurred, based on stoichiometric deficiencies of evolved  $\text{HClO}_4$ , compared to  $\text{NH}_3$ , and also relatively high  $\text{Cl}/\text{N}$  atom balance estimates (not shown) derived from evolved decomposition products.

Inconclusive evidence was found for  $\text{HOClO}_3 \rightarrow \text{HO} \cdot + \text{ClO}_3 \cdot$  proposed by Levy<sup>6</sup> as being rate determining in the homogeneous decomposition of  $\text{HClO}_4$  above  $330^\circ\text{C}$ . In all

four LP systems, conditions were found where 20 eV  $\text{ClO}_3/\text{HClO}_4$  ion ratios significantly exceeded (30–100%) the values of 1.33 and 1.49 obtained from ID of AP at 260 and  $380^\circ\text{C}$ . However, since excess  $\text{ClO}_3$  ion may arise from enhanced fragmentation of  $\text{HClO}_4$  at higher vibrational temperatures, the presence of evolved  $\text{ClO}_3$  was somewhat uncertain. Note that much stronger evidence was recently found for  $\text{ClO}_3$  evolution associated with condensed-phase decomposition (rather than dissociative evaporation) in high-temperature  $\text{CO}_2$  laser pyrolyses of pure AP; however,  $\text{ClO}_2$  was not a major product in this system.<sup>2</sup>

Since  $\text{ClO}_2$  was always a major gaseous product (except at 0.3% carbon black), and was evolved over a much longer duration than  $\text{HClO}_4$  and the aforementioned “trace” of  $\text{ClO}_3$ , it must be considered a primary “quasi-stable” intermediate in the heterogeneous decomposition of  $\text{HClO}_4$ . Since  $\text{Cl}_2$  and  $\text{ClO}$  were always evolved in much smaller quantities than  $\text{ClO}_2$ , and since the thermal decomposition of  $\text{ClO}_2$  (which is rapid at  $50^\circ\text{C}$  and 200 mm Hg<sup>7</sup>) involves some production of  $\text{ClO}$  radicals and obeys the over-all stoichiometry  $2 \text{ClO}_2 \rightarrow \text{Cl}_2 + 2 \text{O}_2$  under a variety of conditions,<sup>8</sup>  $\text{ClO}_2$  decomposition as shown was largely incomplete under LP conditions.

A large portion of the observed  $\text{HCl}$  probably originated from heterogeneous decomposition of  $\text{HClO}_4$ . Indirect support for this is given by mass spectrometer results of Heath and Majer,<sup>9</sup> which indicate that  $\text{HCl}$  was the most abundant ion (70 eV) when  $\text{HClO}_4$  was decomposed heterogeneously on a platinum filament at low pressures and temperatures ranging from “just visibly glowing” at 40 ma to “bright red” at 120 ma.

In the same  $\text{HClO}_4$  decomposition experiments,<sup>9</sup>  $\text{O}_2$  was the second most abundant ion, and  $\text{ClO}_2$  was the third most abundant. Confirmation of the former result in LP of AP/metal oxide mixtures was not possible, since the  $\text{O}_2$  evolved when metal oxides were flashed alone precluded accurate  $\text{O}_2$ -difference determinations. The latter  $\text{ClO}_2$  finding, supported by a more recent detailed study of  $\text{HClO}_4$  decompositions,<sup>10</sup> is felt to be an excellent indirect confirmation of the present LP results.

$\text{NO}$  was always a major product in the AP/metal oxide systems, in contrast to its role as a minor product in ID of AP and also  $\text{CO}_2$  laser pyrolyses of AP.<sup>2</sup> From the ion intensity standpoint the following inequality applied to the nitrogen-containing products in the AP/metal oxide systems:  $\text{NO} \gg \text{N}_2 > \text{N}_2\text{O} > \text{NO}_2$ .  $\text{NO}$  appeared to be comparatively less abundant in the AP/carbon black system than with the metal oxides, which are known to be effective  $\text{NH}_3$  oxidation catalysts.

#### LP of AP Propellant System

A 15% aluminized PBAA/AP propellant was studied with the LP technique in an effort to observe products arising from heterogeneous reactions in a “real” composite system, as shown in Fig. 8. The sample was impacted repeatedly, with progressively increasing energy, using a sequence of transmission filters. Approximately  $20 \mu\text{m}$  aluminum spheres were formed from the  $7 \mu\text{m}$  aluminum powder, within this energy range. Thus the binder matrix attained at least  $660^\circ\text{C}$ . The normalized  $\text{ClO}_2$  and  $\text{NH}_3$  ion intensity ratios were relatively insensitive to impact energy over the range 4–10 cal/cm<sup>2</sup>. The arrow (bottom left) indicates the range of 70 eV  $\text{ClO}_2/\text{HCl}$  ratios found in several LP of AP/carbon black mixtures and AP crystals resting on a solid graphite substrate.  $\text{HClO}_4$  was seen in very small quantities in the PBAA series, as were  $\text{O}_2$ ,  $\text{Cl}_2$ , and  $\text{NO}_2$ . From the ion intensity standpoint, the butadiene monomer appeared to be the major organic product.

#### LP vs ID in Various AP Systems

In order to provide a basic phenomenological comparison between LP and slower bulk decompositions of mixed AP

§ Calculated by subtracting the following 20 eV fragmentation contributions obtained under selected ID and LP conditions where the number of  $\text{ClO}$ -ion sources was minimized:  $\text{ClO}/\text{HClO}_4 = 0.10$ ,  $\text{ClO}/\text{ClO}_2 = 0.38$ , and  $\text{ClO}/\text{HOCl} = 0.15$ .

systems at lower temperatures, additional heated-capillary ID of AP/metal oxide mixtures and AP doped with  $\text{KMnO}_4$  and  $\text{CrO}_4^{2-}$  were run at low external pressure. Both  $\text{ClO}_2$  and  $\text{HOCl}$  were observed as characteristic "heterogeneous products" in all cases.

Further considerations of a possible transition in the dominance of primary heterogeneous reactions led to the correlation in Fig. 9a. The ID of pure AP progressed downward along the arbitrarily drawn line with increasing temperatures, from 205 to 380°C, but LP of AP/carbon black was characterized by  $\text{Cl}_2/\text{HCl}$  ratios about an order of magnitude smaller.

ID of  $\text{CuO} \cdot 2\text{H}_2\text{O}$ ,  $\text{Fe}_2\text{O}_3$ , and  $\text{MnO}_2/\text{AP}$  mixtures, at the one percent addition level, are also shown in Figure 9a. Sample temperatures generally ranged from 250–300°C, and the data are displaced considerably (up and right) from ID of pure AP at the same temperature. A simple explanation of this behavior (high  $\text{Cl}_2/\text{HCl}$  ratio) is that  $\text{Cl}_2$  originated from two sources under these ID conditions, in which the packed capillary functioned somewhat analogous to a porous bed reactor. First,  $\text{Cl}_2$  and  $\text{HCl}$  were evolved as normal condensed-phase decomposition products of AP. Secondly,  $\text{Cl}_2$  was probably formed by relatively slow (compared to LP) heterogeneous oxidation of  $\text{HCl}$  and step-wise decomposition of  $\text{HClO}_4$  on the metal oxide catalysts; i.e., since  $\text{HClO}_4$  and the intermediate  $\text{ClO}_2$  were always observed in significant quantities during ID, some "undetected"  $\text{ClO}_2$  likely decomposed further to  $\text{Cl}_2$  and  $\text{O}_2$ . A similar argument might be applied to the correspondingly high  $\text{NO}_2/\text{HCl}$  ratios, recognizing that additional  $\text{NO}_2$  could result from heterogeneous oxidation of  $\text{NH}_3$  on the metal oxide catalysts at 250–300°C. The ID  $\text{CuO} \cdot 2\text{H}_2\text{O}$  results are in substantial agreement with those of Rosser, Inami, and Wise<sup>5</sup> in that  $\text{Cl}_2$  and  $\text{O}_2$  were major products.

In contrast to the ID results for metal oxide catalyst/AP mixtures, the LP results for these catalysts are clustered in the lower left region of Fig. 9a. Here, both  $\text{NO}_2$  and  $\text{Cl}_2$  were minor products in comparison to the primary heterogeneously produced products  $\text{HCl}$ ,  $\text{ClO}_2$ ,  $\text{H}_2\text{O}$ ,  $\text{NO}$ , and  $\text{HOCl}$ . Catalyst additions over the range of 0.3–50% did not appear to have a significant effect on the applicability of the correlation.

Figure 9a also shows results obtained from AP containing isomorphously substituted  $\text{KMnO}_4$  in 1.06 and 1.68 mole %

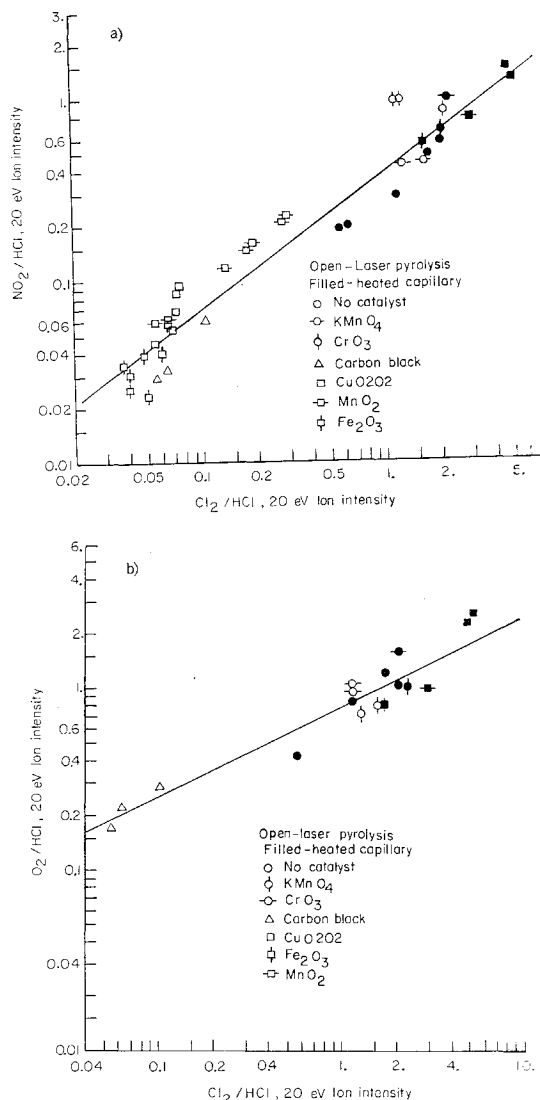


Fig. 9 Some product comparisons between ruby laser and isothermal pyrolyses of various  $\text{NH}_4\text{ClO}_4$  systems which suggest a variable dominance of heterogeneous decomposition pathways, depending on reaction conditions.

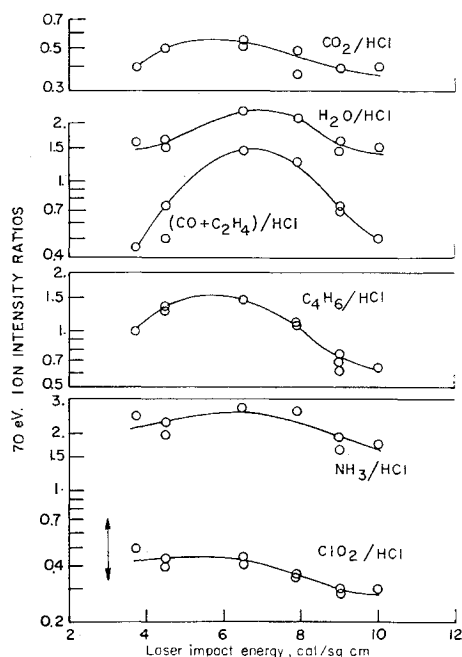


Fig. 8 Ruby laser pyrolyses of a 15% aluminized PBAA/AP propellant.

quantities. The presumably high-temperature LP results (2–6 cal/cm<sup>2</sup>) are located in the same upper right region that characterized an ID result at 185°C. Similar findings are shown for  $\text{CrO}_4^{2-}$  (derived from solution of  $\text{CrO}_3$ ) doped AP.  $\text{ClO}_2$  was always evolved in the respective LP (and ID), but  $\text{ClO}_2/\text{Cl}_2$  appeared to vary somewhat with impact energy and percent additive. Despite relatively high productions of  $\text{Cl}_2$  and  $\text{NO}_2$ , the significant evolutions of  $\text{ClO}_2$  and  $\text{HOCl}$ , and also abnormally high rates of ID were indicative of some "catalyzed behavior," which presumably involved valence changes in the Mn and Cr-containing ions.

The above results lend further, albeit diverse, support for the concept that both the site of  $\text{HClO}_4$  decomposition and the temperature-time history significantly affect the decomposition chemistry. The apparent favoring of  $\text{Cl}_2$  formation when adsorbed  $\text{HClO}_4$  (or possibly a  $\text{NH}_3\text{—H—ClO}_4$  intermediate) decomposes on a "pure" AP crystal surface seems to be in sharp contrast to heterogeneous  $\text{HClO}_4$  decomposition on "catalytic" surfaces, where  $\text{ClO}_2$  is evolved as an intermediate when the effective residence time is short.

The apparent transition of pyrolysis behavior in Fig. 9a, based on the  $\text{NO}_2/\text{HCl}$  and  $\text{Cl}_2/\text{HCl}$  ratios, was also found to apply to  $\text{O}_2/\text{HCl}$  on a limited basis; i.e., LP of AP/metal oxide mixtures were excluded since some  $\text{O}_2$  was evolved when pure metal oxides were flash heated. These results are shown

**Table 1** Product distributions obtained from LP of  $^{15}\text{NH}_4\text{ClO}_4$ /metal oxide mixtures; 20 eV ion intensities

	Cu 0202	$\text{Fe}_2\text{O}_3$	$\text{MnO}_2$
Wt% (estimated)	50	50	70
HCl	1.00	1.00	1.00
$\text{N}_2$	0.20	0.14	0.31
CO	0.2	0.19	0.2
$\text{N}_2\text{O}$	0.11	0.04	0.13
$\text{CO}_2$	0.75	0.57	0.45
NO	0.88	0.67	0.40
$\text{NO}_2$	0.08	0.03	0.06
$\text{ClO}_2$	0.72	0.31	1.65
HOCl	0.30	0.09	0.38
$\text{NH}_3 + \text{H}_2\text{O}$	15	3.3	12.3

in Fig. 9b. Further evidence indicated that  $\text{N}_2\text{O}/\text{HCl}$  also exhibited the same general trend in behavior. This was seen in isothermal decompositions of pure AP in Fig. 4, in LP of  $^{15}\text{NH}_4\text{ClO}_4$ /metal oxide mixtures in Table 1, and in ID of metal oxide/AP mixtures as follows. The 20 eV ( $\text{N}_2\text{O} + \text{CO}_2$ )/HCl ratios were 2.38 and 2.47 for Cu 0202, 1.04 for  $\text{Fe}_2\text{O}_3$ , and 1.15 for  $\text{MnO}_2$ ; all of these indicate substantial  $\text{N}_2\text{O}$  formation after a suitable correction for  $\text{CO}_2$  is applied.

### Summary and Conclusions

Consistent evidence has indicated that in pulsed ruby laser pyrolyses (LP) of AP mixed with finely divided carbon black or metal oxide substrates, the predominant decomposition pathways involved high-temperature heterogeneous reactions. Since open sample geometries and initial pressures below  $10^{-6}$  torr were employed, desorption was favored and gas phase reactions probably had a negligible effect on the product distributions.

The first decomposition step appeared to be proton transfer dissociation of AP into  $\text{NH}_3$  and  $\text{HClO}_4$ . Both were always observed initially, but there was generally a large stoichiometric deficiency of  $\text{HClO}_4$  in the gas phase. Adsorbed  $\text{HClO}_4$  appeared to have undergone a rapid heterogeneous decomposition on the substrate material, wherein  $\text{ClO}_2$  and HCl were evolved in relatively large quantities. Small quantities of  $\text{ClO}_3$  were also detected, suggesting some  $\text{HO}-\text{ClO}_3$  cleavage, but not in the comparatively high abundance found in  $\text{CO}_2$  laser pyrolyses of AP.<sup>2</sup> Relatively little decomposition of the  $\text{ClO}_2$  appeared to occur under LP conditions, since ClO and  $\text{Cl}_2$  were evolved in comparatively small quantities. Chemisorbed oxygen and/or other oxygen carriers such as OH and ClO were most probably formed on the substrate simultaneously, however. These could react with the substrate, as in the case of carbon, and also abstract hydrogen from adsorbed  $\text{NH}_3$  and its dehydrogenated fragments to form  $\text{H}_2\text{O}$  and NO, which were observed as major decomposition products;  $\text{N}_2$ ,  $\text{N}_2\text{O}$ , and  $\text{NO}_2$  were found to be minor products. HOCl was a significant and characteristic product of heterogeneous decomposition, but was generally evolved a few milliseconds after the above products were detected.

Low-pressure isothermal decompositions (ID) of AP, doped AP and AP/substrate mixtures, heated in a glass capillary up to  $380^\circ\text{C}$ , were also presented. Comparisons of results obtained from the two pyrolysis techniques indicated significant differences in product distribution, and hence decomposition mechanism; e.g.,  $\text{ClO}_2$  and HOCl were not products of pure AP decomposition in the present ID, or in high-temperature  $\text{CO}_2$  laser pyrolyses.<sup>2</sup> Further LP vs ID comparisons, in which the  $\text{Cl}_2/\text{HCl}$  ratio varied by two orders of magnitude, provided additional evidence for a transition in pyrolysis behavior relating to the extent of heterogeneous  $\text{HClO}_4$  decomposition. The site of  $\text{HClO}_4$  decomposition appeared to be at least as important as temperature and effective residence

time in determining the predominant chemical pathways.  $\text{CO}_2$ -laser pyrolyses<sup>2</sup> of pure AP,  $\text{KMnO}_4$ -doped AP and AP/metal oxide mixtures at heating rates between 40 and 220  $\text{cal}/\text{cm}^2\text{sec}$  fully support this conclusion.

Results on the flash pyrolysis of AP on graphite substrates, and kinetic spectroscopy of the gaseous products,<sup>11</sup> support the present findings of  $\text{ClO}_2$  and NO formation as major products (in the AP/carbon black and graphite systems). The  $\text{ClO}_2$  attained maximum concentration soon after initiation of the xenon pyrolysis flash ( $<20\mu\text{sec}$ ), and then underwent a rapid photochemical (UV) dissociation into ClO. The NO was formed more slowly, and required more than one msec to attain maximum concentration.

The roles that various chlorine oxides play in the decomposition and combustion of AP are pivotal to our understanding. Unfortunately these compounds are difficult to observe by less direct sampling means because of their high reactivity. Mechanisms based on the probable chlorine oxides have been tentatively formulated to explain the role of  $\text{HClO}_4$  vapor in ignitions of uncatalyzed and catalyzed solid propellant fuels,<sup>12-14</sup> and, more generally, the fate of  $\text{HClO}_4$  and  $\text{NH}_3$  during AP decomposition and combustion under a variety of experimental and practical conditions.<sup>1,15</sup>

### References

- Jacobs, P. W. M. and Whitehead, H. M., "Decomposition and Combustion of Ammonium Perchlorate," *Chemical Reviews*, Vol. 69, 1969, pp. 551-590.
- Pellet, G. L. and Cofer, W. R., III, "High-Temperature Decomposition of Ammonium Perchlorate Using  $\text{CO}_2$  Laser-Mass Spectrometry," AIAA Paper 69-143, New York, 1969.
- Dodé, M., "Sur la Décomposition Thermique du Perchlorate d'Ammonium. II, Partie Experimentale," *Bulletin de la Société Chimique de France*, Vol. 5, 1938, pp. 176-183.
- Bircumshaw, L. L. and Newman, B. H., "The Thermal Decomposition of Ammonium Perchlorate. I, Introduction, Experimental, Analysis of Gaseous Products, and Thermal Decomposition Experiments," *Proceedings of the Royal Society (London)*, Vol. 227A, 1954, pp. 115-132.
- Rosser, W. A., Inami, S. H., and Wise, H., "Kinetics of Decomposition of Ammonium Perchlorate," Rept. PU 3573, Sept. 1966, Office of Naval Research Report under Contract Nonr-3415(00) with Stanford Research Institute.
- Levy, J. B., "The Thermal Decomposition of Perchloric Acid Vapor," *Journal of Physical Chemistry*, Vol. 66, 1962, pp. 1092-1097.
- Schumacher, H. J. and Stieger, G., "The Thermal Decomposition of Chlorine Dioxide," *Zeitschrift für Physikalische Chemie Abt. B. Chemie der Elementarprozesse*, Vol. 7, 1930, pp. 363-186.
- Laffitte, P. et al., "Characteristics of Chlorine Dioxide Decomposition Flames at Reduced Pressures," *11th Symposium (International) on Combustion*, The Combustion Institute, Pittsburgh, 1967, p. 941.
- Heath, G. A. and Majer, J. R., "Mass Spectrometric Study of the Thermal Decomposition of Ammonium Perchlorate," *Transactions of the Faraday Society*, Vol. 60, 1964, pp. 1783-1791.
- Fisher, I. P., "A Mass Spectrometric Study of the Thermal Decomposition of Perchloric Acid and Chlorine Dioxide," TR-66/13, Nov. 1966, Rocket Propulsion Establishment, Westcott, England.
- Petrella, R. V. and Spink, T. L., "Flash Pyrolysis and Kinetic Spectroscopy of Ammonium Perchlorate," *Journal of Chemical Physics*, Vol. 47, 1967, pp. 1488-1490.
- Pearson, G. S. and Sutton, D., "Ignition of Composite Propellant Fuels by Perchloric Acid Vapor," *AIAA Journal*, Vol. 4, 1966, pp. 954-956.
- Pearson, G. S. and Sutton, D., "Composite Solid Propellant Ignition: Ignition of Ammonia and Other Fuels by Perchloric Acid Vapor," *AIAA Journal*, Vol. 5, No. 2, Feb. 1967, pp. 344-346.
- Pearson, G. S. and Sutton, D., "Catalyzed Ignition of Composite Solid Propellant Fuels by Perchloric Acid Vapor," *AIAA Journal*, Vol. 5, No. 11, Nov. 1967, pp. 2101-2103.
- Jacobs, P. W. M. and Pearson, G. S., "Mechanism of the Decomposition of Ammonium Perchlorate," *Combustion and Flame*, Vol. 13, 1969, pp. 419-30.